

## $Q_\beta$ measurements of neutron-rich isotopes with a total-absorption type Ge detector using the KUR-ISOL

Hiroaki Hayashi<sup>1,a</sup>, Itaru Miyazaki<sup>1</sup>, Michihiro Shibata<sup>2</sup>, Yasuaki Kojima<sup>3</sup>, and Akihiro Taniguchi<sup>4</sup>

<sup>1</sup> Graduate School of Engineering, Nagoya University, Nagoya, 464-8603, Japan

<sup>2</sup> Radioisotope Research Center, Nagoya University, Nagoya, 464-8602, Japan

<sup>3</sup> Graduate School of Engineering, Hiroshima University, Higashi-Hiroshima, 739-8527, Japan

<sup>4</sup> Research Reactor Institute, Kyoto University, Sennan-gun, Osaka 590-0494, Japan

**Abstract.** To measure  $Q_\beta$ s of neutron-rich nuclei far from the stability, the total-absorption-type Ge detector has been developed. The detector is composed of a large true-coaxial type HPGe detector and an annular BGO scintillation detector for the Compton suppression. To check the detector performance, nineteen nuclides having precisely measured  $Q_\beta$ s are measured. The nuclei of interest were prepared by  $(n, \gamma)$  reactions and  $^{235}\text{U}(n,f)$  reactions using the Kyoto University Reactor (KUR). The response functions of  $\gamma$ -rays and monoenergetic electrons were calculated by means of the Monte Carlo simulation code (EGS4), and the folding method was used to deduce  $Q_\beta$ s. The nuclei  $^{147-149}\text{La}$ ,  $^{151}\text{Ce}$ , and  $^{153}\text{Pr}$ , for which precise information of the decay schemes were not reported, were prepared by the on-line mass separator (KUR-ISOL) and were measured by the total-absorption type Ge detector. The deduced  $Q_\beta$ s were consistent with preliminarily measured ones by a total absorption BGO detector. The evaluated values by Audi et al. were systematically smaller than the present ones.

### 1 Introduction

The atomic masses are one of the most fundamental physical quantities. Experimentally measured atomic masses of nuclei far from the stability have provided the knowledge of nuclear physics and of various nuclear models, and these measured data support the recent calculation such as nucleosynthesis [1].

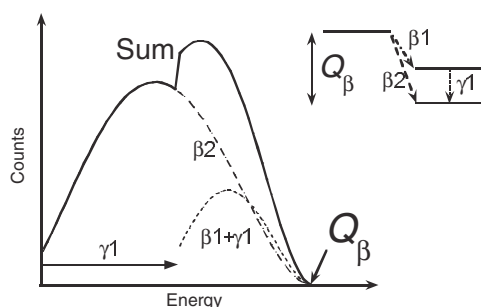


**Fig. 1.** The concept of  $Q_\beta$  measurements using the total absorption detector. An endpoint energy of the obtained spectrum shows the  $Q_\beta$ .

Recently, the evaluated mass table has been provided by Audi et al. [2], and this data table has included measured masses for approximately 2500 nuclides. For the nuclei having no experimental data, atomic masses were deduced by using various mass formulas and systematics. As a result, these data have uncertainties of about 1 MeV. From this fact, the new data for the not yet measured nuclei are important to verify these formulas and the evaluated mass table.

The measure of  $\beta$ -decay energies ( $Q_\beta$ s) is one of the precise measuring ways to deduce atomic masses. Shibata et al.

has developed total absorption BGO detector, and  $Q_\beta$ s of low-yielded nuclei have been reported with accuracy of 100 keV [3–5]. Another type of a total-absorption type Ge detector has been developed. This detector is mainly constructed by an HPGe detector, and more accurate  $Q_\beta$  measurement is expected because of the good energy resolution. In this article, we demonstrate  $Q_\beta$  measurements of neutron-rich nuclei produced with the on-line mass separator installed at the Kyoto University Reactor (KUR-ISOL) [6]. The nuclei  $^{147-149}\text{La}$  and  $^{151}\text{Ce}$ , whose information about the decay schemes has not been precisely reported, were measured.

### 2 Total-absorption type Ge detector

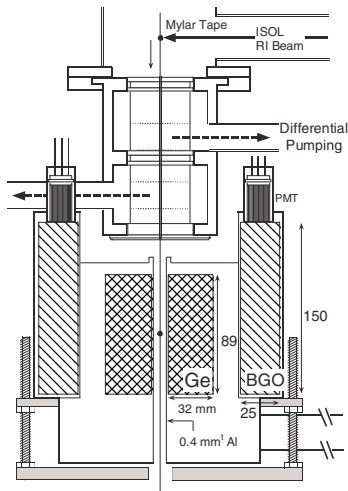
#### 2.1 The concept of $Q_\beta$ measurements using the total absorption detector

Figure 1 shows the concept of the  $Q_\beta$  measurements using the total absorption detector. The detector with a large solid angle absorbs total energies from the radioactivities, as shown in figure 1, the detector can detect an energy of a  $\beta$ -ray ( $\beta_1$ ) to the excited state and of a succeeding  $\gamma$ -ray ( $\gamma_1$ ) together. An endpoint energy of the obtained total absorption spectrum (sum in fig. 1) shows the  $Q_\beta$ , and this fact means the detector can deduce  $Q_\beta$  efficiently without the information of the decay scheme. The detection efficiency of this procedure is approximately 100 times as high as the  $\beta$ - $\gamma$  coincidence method.

#### 2.2 Total-absorption type Ge detector

As shown in figure 2, the total-absorption type Ge detector is composed of a large HPGe detector (diameter of 90 mm

<sup>a</sup> Present author, e-mail: h052304d@mbx.nagoya-u.ac.jp



**Fig. 2.** Schematic view of the total-absorption type Ge detector (installed at KUR-ISOL). The radioactive nuclei are collected on a Mylar tape and periodically transported to the center position of the detector through a differential pumping chamber.

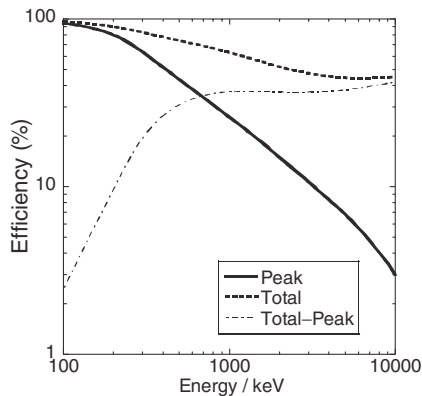


**Fig. 3.** Calculated efficiency curves for  $\gamma$ -ray.

and length of 89 mm) and an annular BGO detector (thickness of 25 mm and length of 150 mm). The HPGe detector is a unique one having a through hole in the center, and radioactive sources can be put into the hole. The inner aluminium housing is very thin (thickness of 0.4 mm) to measure  $\beta$ -rays with low energy losses. The BGO detector is used for detecting Compton scattered  $\gamma$ -rays with a coincidence mode. From geometrical restrictions of the HPGe detector and a beam line of the KUR-ISOL, the HPGe detector could not be covered with the BGO detector completely.

### 2.3 Response function of $\gamma$ -rays

Figure 3 shows calculated efficiency curves for  $\gamma$ -rays. A large Ge crystal and a large solid angle realize high efficiency. However, sufficient efficiencies are not provided for the total absorption detector. The Compton scattered photons, represented by dashed and dotted line (Total-Peak), are approximately 40% for the  $\gamma$ -rays having energies above 1 MeV. From the measured singles spectrum, these distortions have to be removed. Figure 4 shows the measured response function of

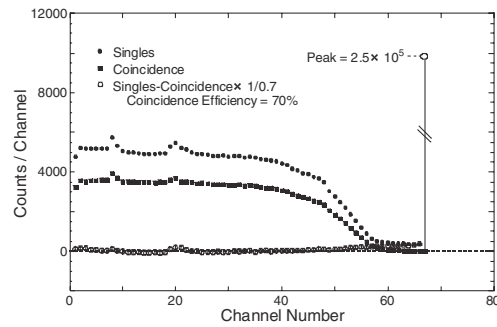


**Fig. 4.** Response function for  $g$ -rays. The effect caused by the Compton scattered photons is reduced by subtracting the coincidence spectrum from singles one.

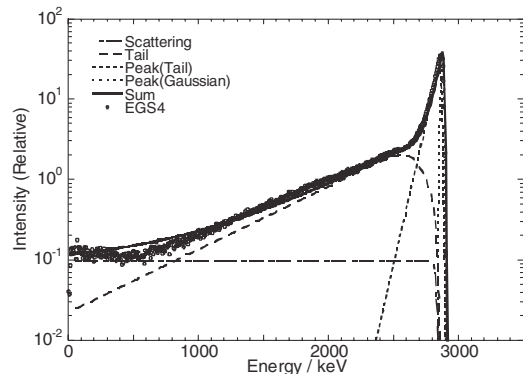


**Fig. 5.** Response function for 3 MeV monoenergetic electron. Using functions, the response functions are divided into three parts (Peak, Tail, Scattering).

the 661 keV  $\gamma$ -ray. Closed circles and closed squares show spectrum of singles and of coincidence between the HPGe detector and the BGO detector, respectively. Here, a total absorption spectrum is obtained by subtracting the coincidence spectrum multiplied by a factor of  $1/\varepsilon$  from the singles one. The factor of  $\varepsilon = 70\%$  means the solid angle of the BGO detector. Open circles of figure 4 show a coincidence subtracted spectrum, and a remaining part in the Compton scattering is less than 6%. The energy dependence of this factor is negligible small according to Monte Carlo simulations calculated by the EGS4 code [7].

### 2.4 Response function of monoenergetic electrons

Response functions for monoenergetic electrons are also needed to analyze measured spectrum. The response functions are calculated by using the EGS4 code [7] from 1–10 MeV. Figure 5 shows a calculated response function for 3 MeV monoenergetic electrons. These response functions were expressed as functions separated into three parts (Peak, Tail, and Scattering). The fitted functions are shown as an example in figure 5. The function is in good agreement with the calculated ones.

The energy dependence of relative intensity of each part for these functions is shown by broken line in figure 6. To verify these functions, the  $^{90}\text{Y}$  spectrum were calculated (folded

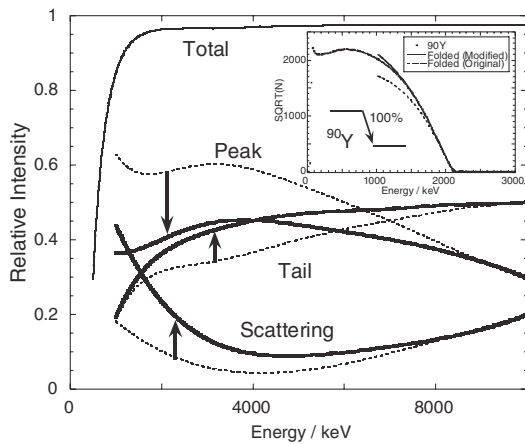


**Fig. 6.** Energy dependence of relative intensity of each part for the response function of monoenergetic electron. The modified response functions (solid lines) are used in the analysis of  $Q_\beta$ s. The inset shows a measured spectrum of  $^{90}\text{Y}$ , compared with folded spectra using modified (solid lines) and original (broken lines) response functions.

these response functions to the theoretical  $\beta$ -ray spectrum), and compared with a measured one. The inset of figure 6 shows the comparison of  $\beta$ -ray spectra. The folded spectrum is deflected from the measured one, so we modified the response functions so as to agree with the measured  $\beta$ -ray spectrum. The modified ratios of response functions and folded spectrum are shown by solid lines. The folded spectrum in the inset of figure 6 is in good agreement with the measured one. A detailed description of these modifications has been reported [8].

### 3 Experiment

Neutron-rich isotopes were produced by thermal neutron induced fission of  $^{235}\text{U}$ . A target chamber was placed in the through-tube facility of the Kyoto University Reactor (KUR). These fission products were separated using on-line mass separator (ISOL) after ionized by a surface ionization type ion source [6]. The mass separated ISOL beams were collected on a Mylar tape in a beam port, and periodically transported to the center position of the total-absorption type Ge detector through a differential pumping chamber (see fig. 2). The cycles of collecting and measuring were set at two or three times as long as half-lives of measured nuclides. By changing these tape cycles and intensities of the ISOL beam, the counting rates were controlled to be below 1500 cps to reduce the pile-up effect. The total-absorption type Ge detector was covered by lead blocks 10 cm thick, by 40% boron-doped rubber sheets 0.5 cm thick and by paraffin blocks 10 cm thick. The background  $\gamma$ -rays were reduced 830 to 120 cps under the reactor and the ISOL operated condition.

To check the detector performances, ten nuclides ( $^{93,95}\text{Sr}$ ,  $^{91-94}\text{Rb}$ ,  $^{139-142}\text{Cs}$ ) having precisely measured  $Q_\beta$ s were measured. These nuclei have  $Q_\beta$ s of 4–10 MeV. Singles and coincidence spectrum were measured during a measuring period of 5–12 hours. Typical measured spectra of  $^{91}\text{Rb}$  are shown in the inset of above right in figure 7 (the background spectrum are subtracted). In addition to this experiment, nine nuclides

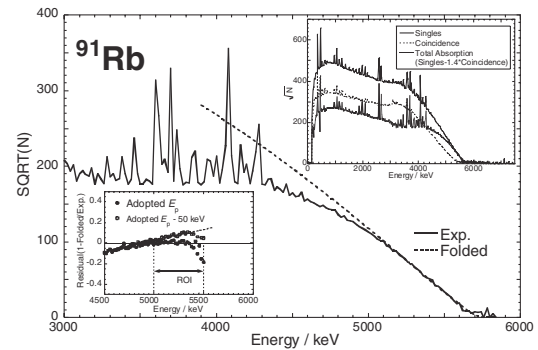


**Fig. 7.** A folded spectrum of  $^{91}\text{Rb}$  compared with a measured one. The inset of top right and bottom left show measured spectra and residual of the spectrum by folded one, respectively.

( $^{27}\text{Mg}$ ,  $^{42}\text{K}$ ,  $^{38}\text{Cl}$ ,  $^{56}\text{Mn}$ ,  $^{52}\text{V}$ ,  $^{72}\text{Ga}$ ,  $^{139}\text{Ba}$ ,  $^{142}\text{Pr}$ , and  $^{90}\text{Y}$ ) were measured. These  $\beta$ -sources have  $Q_\beta$ s of 2–5 MeV and were prepared by thermal neutron irradiation at the KUR, except for  $^{90}\text{Y}$  source. The  $^{90}\text{Y}$  source was made from a commercial source of  $^{90}\text{Sr}$ - $^{90}\text{Y}$ .

The isotopes of  $^{147-149}\text{La}$ ,  $^{151}\text{Ce}$  and  $^{153}\text{Pr}$  were also produced by the ISOL and measured. The  $Q_\beta$ s of these nuclei were previously measured with accuracy of 100 keV by Shibata et al. using a total absorption BGO detector [5] installed at the KUR-ISOL. It is important to measure these nuclei using different detectors to improve reliabilities of the deduced  $Q_\beta$ s. For these nuclei, total counting rates of 10–120 cps were obtained, and measuring period was approximately 10 h for each nuclide.

### 4 Analysis

#### 4.1 $Q_\beta$ determination using the folding method

From the singles spectrum, the coincidence spectrum multiplied by a factor of  $1/\varepsilon$  was subtracted to reduce the effect of Compton scattered  $\gamma$ -rays as described in the section 2.3. Then, the subtracted spectrum was analyzed by folding method and endpoint energy ( $E_p$ ) was deduced. The  $Q_\beta$ s were deduced by correcting the energy losses of electrons to the  $E_p$ s. In this analysis,  $\beta$ -feedings to ground state is assumed, and the theoretical  $\beta$ -ray spectrum of this feeding is folded by the modified response functions of monoenergetic electrons. The figure 7 shows the folded spectrum for  $^{91}\text{Rb}$  compared with the measured one. Taking account of an energy region of 0.5 MeV below an endpoint of the spectrum, the folded spectrum being in agreement with the measured spectrum was searched by changing the parameter of the  $E_p$  in the folded spectrum. As an example in the inset of below left in figure 7, trends of the residuals of the experimental spectrum are checked. It was found that the adopted folded spectra shows the residual of zero crossing and folded spectra given wrong  $E_p$ s show residuals deflected from the zero crossing. Most of nuclides show good agreement in the region of interest (ROI). The statistical uncertainty of the  $E_p$  was estimated by statistical deviations, and the error of  $Q_\beta$  was derived by the statistical uncertainty and systematical one owing to the folding analysis.

## 4.2 Evaluation of the analysis procedure

To compare measured  $E_{ps}$  and the evaluated  $Q_{\beta s}$  by Audi et al. [2], this analysing procedure using the folding method is evaluated. As shown in figure 8, the energy loss of electrons is deduced to be 163 keV by subtracting an evaluated  $Q_{\beta s}$  from the deduced  $E_{ps}$ . Systematic uncertainties of the analysis procedure are evaluated by deviations from the line of the energy loss; they are 20 keV for 2–4 MeV and 40 keV for 5–8 MeV. The  $Q_{\beta}$  of  $^{94}\text{Rb}$  has a large error, because the Ge detector does not have sufficient efficiency for 10 MeV.

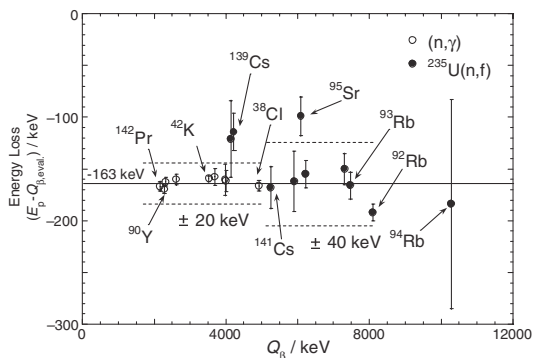


**Fig. 8.** Comparisons between measured  $E_{ps}$  and evaluated  $Q_{\beta s}$ . Systematical uncertainties of the analyzing procedure are evaluated from deviations.

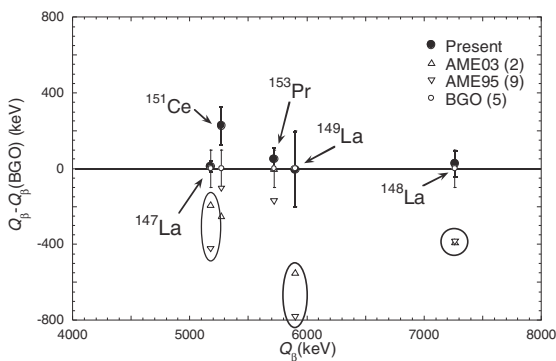


**Fig. 9.** Comparisons of  $Q_{\beta s}$  for  $^{147-149}\text{La}$ ,  $^{151}\text{Ce}$ , and  $^{153}\text{Pr}$ . The evaluated values of La isotopes are systematically smaller than the measured ones.

## 5 Results and discussion

The  $Q_{\beta s}$  of  $^{147-149}\text{La}$ ,  $^{151}\text{Ce}$ , and  $^{153}\text{Pr}$  were deduced using folding method described above. The accuracies of these  $Q_{\beta s}$  were about 100–200 keV. These values are much larger than systematic uncertainties of this energy region, and mainly

caused by statistical uncertainties. Figure 9 shows comparisons of  $Q_{\beta s}$ . The present values are in good agreement with the values measured by total absorption BGO detector [5], in which  $Q_{\beta s}$  were analyzed by a conventional root plot method. It is important that the  $Q_{\beta s}$  deduced by different detector and analyzing procedure are consistent. On the other hand, the evaluated values by Audi et al. (AME03 is ref. [2] and AME95 is ref. [9]) are systematically smaller than the present values. Particularly, the differences of La isotopes are approximately 200–600 keV, and these values are as large as the RMS errors of recently calculated masses of 600 keV [10]. Re-evaluations of these masses are needed.

## 6 Conclusions

The total-absorption type Ge detector has been developed. The response functions of  $\gamma$ -rays and monoenergetic electrons were calculated by the EGS4 code, and the  $Q_{\beta s}$  were analyzed by the folding method. Nineteen nuclides having precisely measured  $Q_{\beta s}$  were measured, and the energy loss of the housing of Ge detector was estimated. The systematic uncertainties of analyzing procedure were evaluated to be 20 keV for 2–4 MeV and 40 keV for 5–8 MeV.

The  $Q_{\beta s}$  of  $^{147-149}\text{La}$ ,  $^{151}\text{Ce}$ , and  $^{153}\text{Pr}$  were measured by the total-absorption type Ge detector installed at the KUR-ISOL. The deduced  $Q_{\beta s}$  were consistent with ones preliminarily measured by the total absorption BGO detector. The evaluated values by Audi et al. were systematically smaller than the present ones.

## References

1. S.E. Woosley and Thomas A. Weaver, *Ann. Rev. Astron. Astrophys.* **24**, 205 (1986).
2. G. Audi, A.H. Wapstra, C. Thibault, *Nucl. Phys. A* **729**, 337 (2003).
3. M. Shibata, Y. Kojima, H. Uno, K. Kawase, A. Taniguchi, Y. Kawase, S. Ichikawa, F. Maekawa, Y. Ikeda, *Nucl. Instrum. Meth. A* **459**, 581 (2001).
4. M. Shibata, T. Shindo, A. Taniguchi, Y. Kojima, K. Kawade, S. Ichikawa, Y. Kawase, *J. Phys. Soc. Jpn.* **71**, 1401 (2002).
5. M. Shibata, O. Suematsu, K. Kawade, M. Asai, S. Ichikawa, Y. Nagame, A. Osa, K. Tsukada, Y. Kojima, A. Taniguchi, *Proceedings of the Third International Conference "Fission and properties of neutron-rich nuclei"* (2002), p. 233.
6. A. Taniguchi, K. Okano, T. Sharshar, Y. Kawase, *Nucl. Instrum. Meth. A* **351**, 378 (1994).
7. W.R. Nelson, H. Hirayama, D.W.O. Rogers, SLAC-245, Stanford Linear Accelerator Center (1985).
8. H. Hayashi, I. Miyazaki, M. Shibata, K. Kawade, Y. Kojima, A. Taniguchi, *Proceedings of the Third International Workshop on EGS* (KEK proceedings 2005-3) (2004), p. 237.
9. G. Audi, A.H. Wapstra, *Nucl. Phys. A* **595**, 409 (1995).
10. H. Koura, T. Tachibana, M. Uno, M. Yamada, *Prog. Theor. Phys.*, Vol. **113**, No. 2, 305 (2005).